Long-Range Entanglement near a Kondo-Destruction Quantum Critical Point

Christopher Wagner, Tathagata Chowdhury, J. H. Pixley, and Kevin Ingersent

Phys. Rev. Lett. **121**, 147602 — Published 5 October 2018

DOI: 10.1103/PhysRevLett.121.147602

Long-range entanglement near a Kondo-destruction quantum critical point

Christopher Wagner,[1] Tathagata Chowdhury,[1,2] J. H. Pixley,[3,4] and Kevin Ingersent[1]

[1] *Department of Physics, University of Florida, Gainesville, Florida 32611-8440, USA*
[2] *Institut für Theoretische Physik, Universität zu Köln, Zülpicher Strasse 77a, 507937 Köln, Germany*
[3] *Department of Physics and Astronomy, Center for Materials Theory, Rutgers University, Piscataway, NJ 08854 USA*
[4] *Condensed Matter Theory Center and the Joint Quantum Institute, Department of Physics, University of Maryland, College Park, Maryland 20742-4111, USA*

(Dated: September 4, 2018)

The numerical renormalization group is used to study quantum entanglement in the Kondo impurity model with a density of states $\rho(\varepsilon) \propto |\varepsilon|^r$ $(0 < r < \frac{1}{2})$ that vanishes at the Fermi energy $\varepsilon = 0$. This nonintegrable model features a Kondo-destruction quantum critical point (QCP) separating a partially screened phase from a local-moment phase. The impurity contribution $S_e^{\rm imp}$ to the entanglement entropy between a region of radius R around the magnetic impurity and the rest of the system reveals a length scale R^* that distinguishes a region $R \ll R^*$ of strong critical entanglement from one $R \gg R^*$ of weak entanglement. Within each phase, $S_e^{\rm imp}$ is a universal function of R/R^* with power-law decay for $R/R^* \gg 1$. The entanglement length R^* diverges on approach to the interacting QCP, showing that the critical Kondo screening cloud subsumes the entire system as the impurity becomes maximally entangled with the conduction band. This work has implications for entanglement calculations in other models and for the nature of heavy-fermion quantum criticality.

Quantification of entanglement [1] has helped develop new fundamental concepts in condensed matter physics [2]. The entanglement entropy $S_e \geq 0$ characterizes a pure state of a system with respect to partition into subsystems A and B: if $S_e > 0$, a measurement that collapses the state of A must also collapse B. Entanglement has recently been measured in ultra-cold atomic gases [3], making it experimentally relevant to ask how S_e scales with the length l of the smaller subsystem in d spatial dimensions. Certain eigenstates can be classified by an "area law" $S_e \sim l^{d-1}$ (e.g., describing various ground states [4]) or a "volume law" $S_e \sim l^d$ (typical for highly excited states in a thermal system [5]). The existence of a Fermi surface can impart a logarithmic area-law correction: $S_e \sim l^{d-1} \log l$ [6]. In more exotic phases lacking a local order parameter, $S_e = al - \gamma + \ldots$ describes a long-range-entangled ground state with a universal area-law offset γ due to topological order in $d = 2$ [7, 8].

Entanglement entropy has been particularly successful at characterizing ground states of quantum impurity systems, in which a local dynamical degree of freedom entangles with a dense set of host energy levels. For example, the Kondo effect in metals is an inherently quantum-mechanical phenomenon due to its singlet ground state [9]. The natural expectation that the size of the Kondo screening cloud dictates the spatial range of entanglement has been confirmed in the Kondo [10] and related [11, 12] models. However, in situations where the Kondo effect breaks down at a continuous quantum phase transition [13–27], the spatial structure of Kondo screening is poorly understood. Is entanglement long ranged near the quantum critical point (QCP), despite the impurity becoming asymptotically free in the Kondo-destroyed phase? This question is relevant for heavy-fermion compounds—such as $CeCu_{6-x}Au_x$ [28], $YbRh_2Si_2$ [29] and $CeRhIn_5$ [30]—believed to exhibit a Kondo-destruction QCP concomitant with a jump in the Fermi-surface volume. Within an extended dynamical mean-field theory, the universal aspects of the critical destruction of the Kondo effect can be captured by mapping the lattice to an effective impurity model [31]. Thus, entanglement studies of impurity QCPs can provide valuable insights into bulk quantum criticality.

We show that the numerical renormalization group (NRG) can accurately determine the spatial entanglement structure in the ground state of a magnetic impurity in a metal or semimetal. Prior work has investigated the "local" entanglement entropy, taking the impurity alone to form subsystem A [27, 32]. Here, we compute $S_e^{\rm imp}(R)$, the impurity contribution to the entanglement entropy between a region of radius R about the impurity and the rest of the system. In a metal, where the impurity spin becomes fully screened at temperatures $T \ll T_K$ (the Kondo temperature), we confirm the previously deduced [10–12] scaling of $S_e^{\rm imp}$ with R/R_K, where $R_K \propto 1/T_K$ is believed to be the characteristic size of the Kondo cloud.

Our main results are for the nonintegrable pseudogap Kondo model [13], where a Kondo-destruction QCP separates a Kondo phase from a local-moment phase having no *static* Kondo effect. This is one of very few problems where it has proved possible to quantify entanglement near an interacting QCP without approximation or bias. Each phase reveals a length scale R^* such that for $R \ll R^*$, $S_e^{\rm imp}$ takes its maximum value, signaling strong entanglement associated with criticality. In the Kondo phase, $S_e^{\rm imp}$ decreases for $R \gg R^*$, but (in contrast to the metallic case) remains nonzero for $R \to \infty$ due to incomplete impurity screening [15]. In the local-moment phase, the strong entanglement for $R \ll R^*$ evidences a *dynamical* Kondo effect, but $S_e^{\rm imp} \to 0$ for $R \gg R^*$.

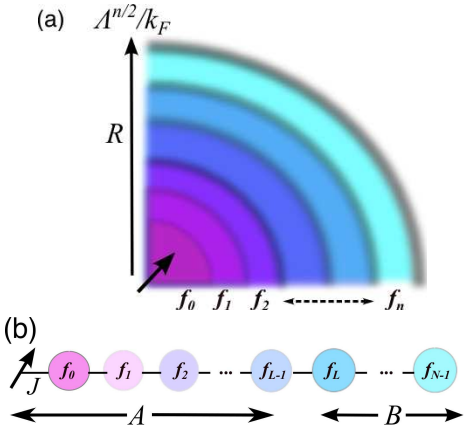

FIG. 1. NRG representation of the Kondo model as a tight-binding Wilson chain of N sites coupled at one end to an impurity spin. (a) In real space, Wilson site n corresponds to a spherically symmetric band state with a radial probabilty density peaked at a radius $\propto k_F^{-1}\Lambda^{n/2}$ from the impurity. (b) The entanglement entropy $S_e(J,L,N)$ is found by splitting the mapped system into subsystems A (the impurity and the first L Wilson sites) and B (the remaining $N-L$ sites).

In each phase, $S_e^{\rm imp}$ is a universal function of R/R^* with power-law decay for $R/R^* \gg 1$. R^* diverges on approach to the QCP, leading to a maximal, scale-invariant entanglement extending throughout the host, implying that the critical Kondo cloud subsumes the entire conduction band. We expect similar behavior to hold near the bulk Kondo-destruction QCPs in heavy-fermion compounds.

Model. The spin-$\frac{1}{2}$ Kondo Hamiltonian is

$$H = \sum_{\mathbf{k},\sigma} \varepsilon_{\mathbf{k}}\, c^\dagger_{\mathbf{k}\sigma}\, c_{\mathbf{k}\sigma} + \frac{J}{2N_{\mathbf{k}}}\, \mathbf{S}_{\rm imp}\cdot \sum_{\mathbf{k},\mathbf{k}',\sigma,\sigma'} c^\dagger_{\mathbf{k}\sigma}\, \boldsymbol{\sigma}_{\sigma\sigma'}\, c_{\mathbf{k}'\sigma'}, \quad (1)$$

where $c_{\mathbf{k}\sigma}$ destroys a band electron of wave vector $\mathbf{k}$, energy $\varepsilon_{\mathbf{k}}$, and spin component $\sigma = \pm\frac{1}{2}$; $N_{\mathbf{k}}$ is the number of host unit cells; J is the local exchange between band electrons and the impurity spin $\mathbf{S}_{\rm imp}$; and $\boldsymbol{\sigma}$ is a vector of Pauli matrices. We use a (simplified) density of states

$$\rho(\varepsilon) = N_{\mathbf{k}}^{-1} \sum_{\mathbf{k}} \delta(\varepsilon - \varepsilon_{\mathbf{k}}) = \rho_0 |\varepsilon/D|^r \Theta(D-|\varepsilon|), \quad (2)$$

D being the half-bandwidth and $\Theta(x)$ the Heaviside function. The model has a rich phase diagram that crucially depends on the band exponent r [15]: $r=0$ corresponds to the integrable Kondo problem in a metal [9], while the semimetallic case $0<r<\frac{1}{2}$ is nonintegrable and features an interacting Kondo-destruction QCP at $J=J_c>0$ at which a critical impurity spin response is characterized by nontrivial, r-dependent exponents [16].

We consider the impurity entanglement entropy $S_e^{\rm imp}(J,R) \equiv S_e(J,R) - S_e^{(0)}(R)$, where $S_e(J,R)$ is the entanglement entropy of the combined impurity-band system with subsystem A consisting of the impurity plus that part of the band within radius R of the impurity site, and $S_e^{(0)}(R)$ is the entanglement entropy of the band alone when partitioned at the same radius [see Fig. 1(a)]. Since the exchange term in Eq. (1) is spherically symmetric, the impurity affects only s-wave band degrees of freedom, and for purposes of calculating impurity-induced properties, the problem reduces to one (radial) dimension. One then has [6, 33, 34] $S_e^{(0)}(R) \sim \log R$ rather than the full three-dimensional behavior $S_e^{(0)}(R) \sim R^2 \log R$.

Method. We study Eq. (1) using the NRG [35, 36] as modified to treat a power-law density of states [15]. The band is mapped onto a semi-infinite tight-binding "Wilson chain" of sites labeled $n = 0, 1, 2, \ldots$, coupled to the impurity via site 0 only. A discretization parameter $\Lambda > 1$ introduces a separation of energy scales that causes the nearest-neighbor hopping to decay as $t_n \sim D\Lambda^{-n/2}$ and allows iterative diagonalization of Kondo Hamiltonians H_M on finite Wilson chains of length $M = 1, 2, \ldots, N$, where N is sufficiently large that t_N is much smaller than any energy of physical interest.

The system described by H_N can be divided into a subsystem A comprising the impurity and the first L chain sites and a subsystem B containing the rest of the chain [Fig. 1(b)]. We use the NRG solutions of H_M with $L \le M \le N$ to compute the reduced density operator $\rho_A = {\rm Tr}_B \rho$ [37–40]. Here, $\rho \propto \exp(-H_N/k_BT)$ is the full density operator at temperature $T \sim t_N/k_B$ so that $S_e(J,L,N) = -{\rm Tr}_A(\rho_A \ln \rho_A)$ is the ground-state entanglement [41]. We also calculate the entanglement entropy $S_e^{(0)}(L,N)$ for the chain alone. Both $S_e(J,L,N)$ and $S_e^{(0)}(L,N)$ become independent of N for $N \gg L$ but include terms proportional to $(-1)^L$ that decay only slowly with increasing L [11, 42]. We therefore focus on smoothed three-point averages $S_e(J,L)$ and $S_e^{(0)}(L)$, defining $S_e^{\rm imp}(J,L)$ to be their difference. Interestingly, even though the host exhibits conformal symmetry only for $r=0$, in the continuum limit $\Lambda \to 1$ with $1 \ll L \ll N$, we recover for any r the result for a critical conformal field theory, $S_e^{(0)}(L,N) = (c/6)\ln L + b$, with an effective central charge $c=2$ [40].

To find $S_e^{\rm imp}$ vs R, we recall [43] that Wilson chain site n has a single-electron wave function $\psi_n(r')$ with greatest radial probability density at radius $r'_n \simeq \eta\Lambda^{n/2}/k_F$, where k_F is the Fermi wave vector and η is of order unity [see Fig. 1(a)]. In the continuum limit $\Lambda \to 1$ and $N \to \infty$, $\psi_n(r')$ approaches a radial delta function. For $\Lambda > 1$, we still expect $S_e^{\rm imp}(J,L)$ to well approximate $S_e^{\rm imp}(J, R = \eta\Lambda^{L/2}/k_F)$. We present NRG results obtained using $\Lambda = 3$, retaining up to 600 many-body eigenstates after each iteration to reach a Wilson chain of $N = 161$ sites. We choose $\eta = 2\Lambda^{1/2}/(\Lambda+1)$ [43] and employ units where $D = \hbar = k_B = 1$.

Results for metallic hosts. Figure 2(a) plots $S_e^{\rm imp}$ vs L for the conventional ($r=0$) Kondo model with different couplings J. For all but the largest J values, $S_e^{\rm imp}$

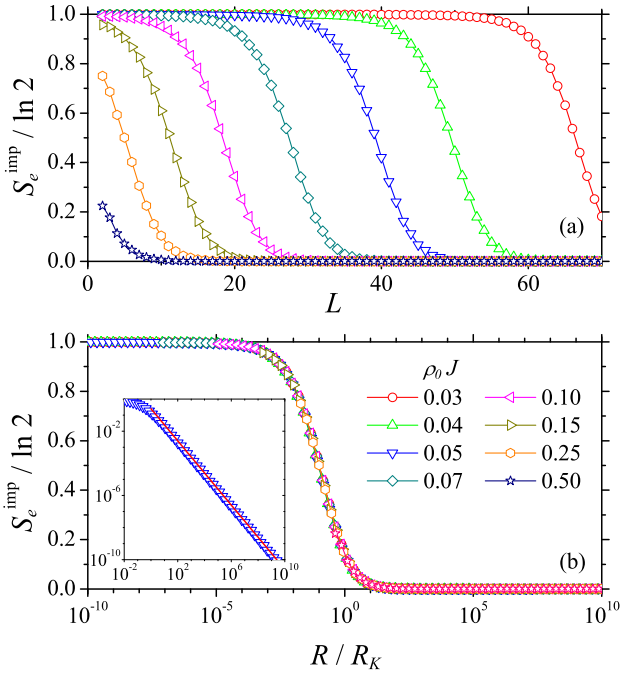

FIG. 2. (a) Impurity entanglement entropy $S_e^{\rm imp}$ vs Wilson chain partition size L for a metallic host ($r = 0$) and different Kondo couplings J labeled in the legend of (b). Lines are guides to the eye. (b) Data from (a) replotted as $S_e^{\rm imp}$ vs R/R_K, where $R = \eta\Lambda^{L/2}/k_F$ and $R_K = 1/(k_F T_K)$ with T_K being the Kondo temperature extracted from the magnetic susceptibility [40]. The collapse of data for different J values points to a one-parameter scaling $S_e^{\rm imp}(J, R) = f_0(R/R_K)$. Inset: Data from main panel for $\rho_0 J = 0.05$ replotted on a log-log scale showing an $(R/R_K)^{-1}$ tail (fitted line) for $R \gg R_K$.

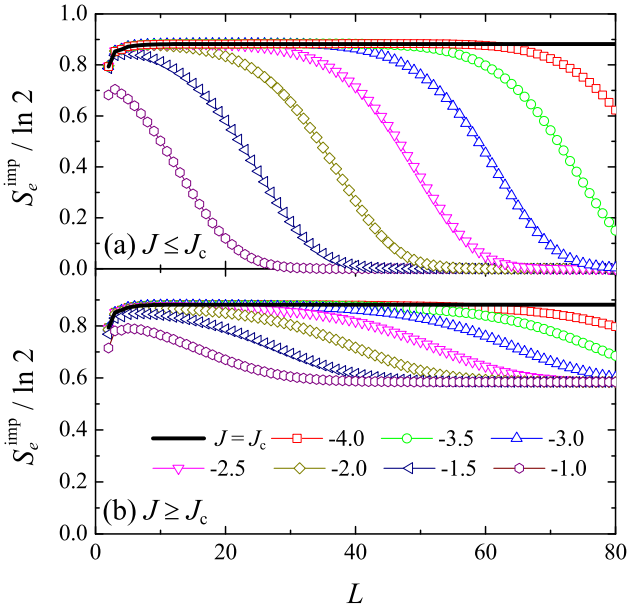

FIG. 3. Impurity entanglement entropy $S_e^{\rm imp}$ vs Wilson chain partition size L for a pseudogap Kondo model with band exponent $r = 0.4$. Symbols plot data for (a) $J = (1 - 10^x)J_c$, and (b) $J = (1+10^x)J_c$, with values of x shown in the legend. Thick lines show the critical case $J = J_c$.

starts for small L at the value $\ln 2$ indicative of a singlet formed between (i) a spin $\frac{1}{2}$ arising from an impurity that is negligibly screened by electrons occupying Wilson sites $n < L$, and (ii) a net spin $\frac{1}{2}$ representing the part of the Kondo screening cloud residing on Wilson chain sites $n \geq L$. For large L, $S_e^{\rm imp}$ approaches zero from above, indicating that the impurity is being Kondo-screened almost entirely by electrons within subsystem A, leaving an entanglement with subsystem B no greater than in the absence of the impurity.

It is natural to associate the crossover from $S_e^{\rm imp} \simeq \ln 2$ to $S_e^{\rm imp} = 0$ with the renormalization-group (RG) flow from weak to strong coupling, known from much previous work [9] to be characterized by a single energy scale T_K. Accordingly, the entanglement is believed [11] to have just one length scale $R_K \simeq 1/(k_F T_K)$. Figure 2(b) replots data from Fig. 2(a) as $S_e^{\rm imp}$ vs R/R_K, revealing an excellent collapse of results for different J and the existence of a universal scaling $S_e^{\rm imp}(J, R) = f_0(R/R_K)$. For $R/R_K \gg 1$, $S_e^{\rm imp}$ decays like $(R/R_K)^{-1}$ [see inset to Fig. 2(b)], consistent with studies of spin chains [11] and a resonant-level model [44].

Results for pseudogapped hosts. We focus on entanglement near the Kondo-destruction QCPs that occur for semimetallic densities of states described by exponents $0 < r < \frac{1}{2}$. Figure 3 illustrates for $r = 0.4$ the variation of $S_e^{\rm imp}$ with Wilson chain partition size L for values of J close to J_c. In the local-moment phase [$J < J_c$, Fig. 3(a)], $S_e^{\rm imp}$ initially rises with increasing L to reach a plateau maximum, only to fall toward zero for larger partition sizes. These data show that even though the impurity spin asymptotically decouples from the band, the impurity induces additional entanglement for finite values of L (or equivalently, at finite energies $\simeq \pm D\Lambda^{-L/2}$), manifesting a *dynamical* Kondo effect.

In the Kondo phase ($J > J_c$), $S_e^{\rm imp}$ again initially rises with increasing L to reach the same plateau maximum before decreasing for larger L values [Fig. 3(b)]. Here, however, the impurity induces an additional entanglement that remains nonzero as $L \to \infty$. This is consistent with the nonvanishing $T \to 0$ limits of both the impurity entropy and the effective magnetic moment, which suggest that the impurity degree of freedom is only partially screened in the pseudogap Kondo phase [15].

Figure 3 also shows that in either phase, $S_e^{\rm imp}$ remains near its plateau maximum to larger values of L the closer J approaches J_c. We are thus led to one of our principal conclusions: At the QCP [thick lines in Figs. 3(a) and 3(b)], the *entire* conduction band is maximally entangled with the impurity, i.e., the ground state has long-range,

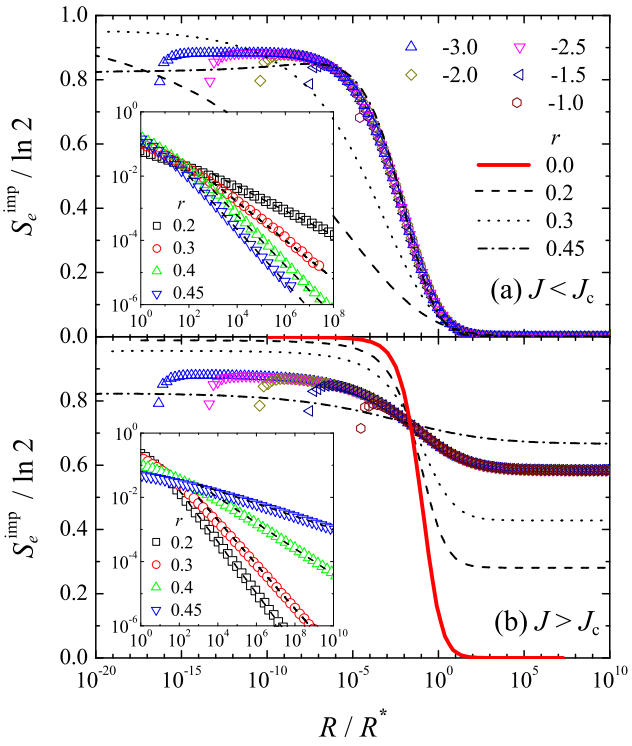

FIG. 4. Data from Fig. 3 replotted vs R/R^*, where $R = \eta\Lambda^{L/2}/k_F$ and $R^* = 1/(k_F T^*)$ with T^* being a crossover temperature scale extracted from the magnetic susceptibility [40]. Symbols plot data for (a) $J = (1-10^x)J_c$, and (b) $J = (1+10^x)J_c$ with values of x labeled in the legend. Lines show fits to data points (not shown) obtained for other values of r. Insets: Log-log plots of large-R data for $S_e^{\rm imp}(J,R) - S_e^{\rm imp}(J,\infty)$ vs R/R^*, calculated for a single Kondo coupling (a) $J < J_c$, (b) $J > J_c$ at each of four different band exponents $r > 0$, with power-law fits (dashed lines).

scale-invariant entanglement.

The preceding picture implies that the eventual decrease in $S_e^{\rm imp}$ vs L for $J \neq J_c$ reflects the RG flow away from the QCP, characterized by a crossover temperature scale $T^* \propto |J - J_c|^\nu$, where $\nu(r)$ is the correlation-length exponent [16]. Following the same reasoning as for a metallic host, we expect T^* to be associated with a length scale $R^* = 1/(k_F T^*)$. Figure 4 replots the $r = 0.4$ data from Fig. 3 as $S_e^{\rm imp}$ vs R/R^* using values of T^* extracted from the magnetic susceptibility [15, 40]. The collapse of data for different J points to the existence of scaling functions $f_r^\pm$ such that

$$S_e^{\rm imp}(J,R) = f_r^\pm(R/R^*) \quad \text{for} \quad J \gtrless J_c. \tag{3}$$

Significant departures from scaling are seen only for the smallest values of R, corresponding to the smallest L in Fig. 3, and can be attributed to the NRG discretization. Figure 4 also plots fitting curves from similar data collapses for band exponents $r = 0.2$, $r = 0.3$ and $r = 0.45$ [45], as well as [in panel (b)] the metallic case $r = 0$.

Whereas in the local-moment phase $S_e^{\rm imp} \to 0$ for $R/R^* \to \infty$, in the Kondo phase $S_e^{\rm imp}$ approaches for $R/R^* \gg 1$ a value that is well-approximated by $S_e^{\rm imp} \simeq \frac{3}{2} r \ln 2$ [40]. Insets in Fig. 4 show that in either phase, the impurity entanglement entropy has a power-law tail

$$S_e^{\rm imp}(J,R) - S_e^{\rm imp}(J,\infty) \propto (R/R^*)^{-\alpha} \quad \text{for } R \gg R^*. \tag{4}$$

Fitted exponents are consistent with $\alpha = 2r$ for $J < J_c$ and $\alpha = \min(1\text{–}r,\ 2\text{–}4r)$ for $J > J_c$, values that represent twice the dimension of the leading irrelevant operator at the local-moment and Kondo fixed points, respectively [40]. This observation is consistent with the interpretation that the power-law tails are associated with the RG flow toward a stable fixed point.

Discussion. We have elucidated the spatial entanglement structure in a family of Kondo models. The impurity entanglement entropy $S_e^{\rm imp}(R)$ for a partition at radius R around a magnetic impurity depends only on R divided by $R^* \propto 1/T^*$, with power-law decay for $R \gg R^*$. In a metal, T^* is the Kondo temperature and R^* is always finite. In a semimetal, the many-body scale T^* vanishes like $|J - J_c|^\nu$ on approach to an interacting QCP so $S_e^{\rm imp}(R)$ becomes infinite ranged and scale invariant; the impurity imparts to the *total* entanglement $S_e = (2/6)\ln R + S_e^{\rm imp}$ a universal critical offset independent of the area of the subsystem boundary, reminiscent of certain 2D topological phases [7, 8]. These results were obtained near a particle-hole-symmetric QCP, but we expect similar behavior at the asymmetric interacting QCPs that arise for $0.375 \lesssim r < 1$ upon addition of potential scattering to Eq. (1) [15].

This work opens a way to study the entanglement structure in more general (e.g., multiband and/or dissipative bosonic) impurity models, both in and out of [39] equilibrium, and in correlated lattice models treated within dynamical mean-field theory [46]. In any Kondo-destroyed phase, despite suppression of static screening, we expect a dynamical Kondo effect to entangle the system over a range that diverges on approach to the Kondo phase boundary. On a technical level, this implies that the ground state cannot be adequately described by a static slave-boson amplitude [47]; dynamical effects must be accounted for. Our findings also suggest that the Kondo-destruction QCP observed in heavy fermions is accompanied by long-range entanglement between all local moments and the entire conduction band. Future work should pursue a connection between this scale-invariant entanglement and the reconstruction of critical Fermi surfaces.

Acknowledgments. We thank Andreas Ludwig and Andrew Mitchell for useful discussions and Seung-Sup Lee for drawing our attention to Ref. 10. This work was supported in part by NSF Grant No. DMR-1508122 (C.W., T.C., and K.I.), by the DFG within the CRC 1238 (Project C03) (T.C.), and by the Laboratory for Physical Sciences (J.H.P). The work of K.I. and J.H.P. was

performed in part at the Aspen Center for Physics, supported by NSF Grants No. PHY-1066293 and No. PHY-1607611. J.H.P. acknowledges the hospitality of the University of Florida.

[1] D. Janzing, in *Compendium of Quantum Physics*, ed. by D. Greenberger, K. Hentschel, and F. Weinert (Springer Berlin Heidelberg, Berlin, Heidelberg, 2009), pp. 205–209.

[2] L. Amico, R. Fazio, A. Osterloh, and V. Vedral, Rev. Mod. Phys. **80**, 517 (2008).

[3] R. Islam *et al.*, Nature (London) **528**, 77 (2015).

[4] J. Eisert, M. Cramer, and M. B. Plenio, Rev. Mod. Phys. **82**, 277 (2010).

[5] R. Nandkishore and D. A. Huse, Ann. Rev. Condens. Matt. Phys. **6**, 15 (2014).

[6] D. Gioev and I. Klich, Phys. Rev. Lett. **96**, 100503 (2006).

[7] A. Kitaev and J. Preskill, Phys. Rev. Lett. **96**, 110404 (2006).

[8] M. Levin and X.G. Wen Phys. Rev. Lett. **96**, 110405 (2006). Nat. Phys. 7, 772 (2011).

[9] A. C. Hewson, *The Kondo Problem to Heavy Fermions* (Cambridge Univ. Press, Cambridge, UK, 1993).

[10] S.-S. B. Lee, J. Park, and H.-S. Sim, Phys. Rev. Lett. **114**, 057203 (2015).

[11] E. S. Sørensen, M.-S. Chang, N. Laflorencie, and I. Affleck, J. Stat. Mech. **2007**, L01001 (2007).

[12] I. Affleck, N. Laflorencie, and E. S. Sørensen, J. Phys. A **42**, 504009 (2009).

[13] D. Withoff and E. Fradkin, Phys. Rev. Lett. **64**, 1835 (1990).

[14] R. Bulla, T. Pruschke, and A. C. Hewson, J. Phys.: Condens. Matt. **9**, 10463 (1997).

[15] C. Gonzalez-Buxton and K. Ingersent, Phys. Rev. B **57**, 14254 (1998).

[16] K. Ingersent and Q. Si, Phys. Rev. Lett. **89**, 076403 (2002).

[17] L. Fritz and M. Vojta, Phys. Rev. B **70**, 214427 (2004).

[18] M. T. Glossop, S. Kirchner, J. H. Pixley, and Q. Si, Phys. Rev. Lett. **107**, 076404 (2011).

[19] I. Schneider, L. Fritz, F. B. Anders, A. Benlagra, and M. Vojta, Phys. Rev. B **84**, 125139 (2011).

[20] J. H. Pixley, S. Kirchner, K. Ingersent, and Q. Si, Phys. Rev. Lett. **109**, 086403 (2012).

[21] A. M. Sengupta, Phys. Rev. B **61**, 4041 (2000).

[22] L. Zhu and Q. Si, Phys. Rev. B **66**, 024426 (2002).

[23] G. Zaránd and E. Demler, Phys. Rev. B **66**, 024427 (2002).

[24] M. Kirćan and M. Vojta, Phys. Rev. B **69**, 174421 (2004).

[25] M. T. Glossop and K. Ingersent, Phys. Rev. Lett. **95**, 067202 (2005).

[26] M. T. Glossop and K. Ingersent, Phys. Rev. B **75**, 104410 (2007).

[27] J. H. Pixley, T. Chowdhury, M. T. Miecnikowski, J. Stephens, C. Wagner, and K. Ingersent, Phys. Rev. B **91**, 245122 (2015).

[28] A. Schröder *et al.*, Nature (London) **407**, 351 (2000).

[29] S. Paschen *et al.*, J. Magn. Magn. Mat. **400**, 17 (2016).

[30] H. Shishido, R. Settai, H. Harima, and Y. Onuki, J. Phys. Soc. Jpn. **74**, 1103 (2005).

[31] Q. Si, S. Rabello, K. Ingersent, and J. L. Smith, Nature (London) **413**, 804 (2001).

[32] For related work on the spin-boson model, see: K. Le Hur, P. Doucet-Beaupré, and W. Hofstetter, Phys. Rev. Lett. **99**, 126801 (2007); A. Kopp and K. Le Hur, Phys. Rev. Lett. **98**, 220401 (2007); K. Le Hur, Ann. Phys. (N.Y.) **323**, 2208 (2008).

[33] B. Swingle, Phys. Rev. Lett. **105**, 050502 (2010).

[34] W. Ding, A. Seidel, and K. Yang, Phys. Rev. X **2**, 011012 (2012).

[35] K. G. Wilson, Rev. Mod. Phys. **47**, 773 (1975).

[36] R. Bulla, T. A. Costi, and T. Pruschke, Rev. Mod. Phys. **80**, 395 (2008).

[37] A. Weichselbaum and J. von Delft, Phys. Rev. Lett. **99**, 076402 (2007).

[38] L. Merker, A. Weichselbaum, and T. A. Costi, Phys. Rev. B **86**, 075153 (2012).

[39] H. T. M. Nghiem and T. A. Costi, Phys. Rev. B **89**, 075118 (2014); *ibid.* **90**, 035129 (2014); arXiv:1803.04098 (unpublished).

[40] See the Supplemental Material at [URL will be provided by publisher] for technical details and additional results, which includes Refs. [48–51].

[41] For $J < J_c$, a tiny magnetic field is introduced to remove a spurious contribution to S_e from the two-fold ground-state degeneracy; see Ref. 27.

[42] Reference 27 studied $S_e^{\rm imp}(J, 0, N)$, which is not directly comparable with the extrapolation to $L = 0$ of the smoothed quantity $S_e^{\rm imp}(J, L)$ discussed in this work.

[43] H. R. Krishna-murthy, J. W. Wilkins, and K. G. Wilson, Phys. Rev. B **21**, 1003 (1980).

[44] H. Saleur, P. Schmitteckert, and R. Vasseur, Phys. Rev. B **88**, 085413 (2013).

[45] For $r = 0.2$ and 0.3, the crossover in $S_e^{\rm imp}$ between its critical and stable fixed-point values is centered at smaller R/R^* for $J < J_c$ than for $J > J_c$. This is an artifact of an impurity magnetization $\langle S^z_{\rm imp}\rangle \sim |h|^{1/\delta}$ induced near $J = J_c$ by the small magnetic field h applied to lift the local-moment ground-state degeneracy. In our quadruple-precision runs, the smallest field that we can use is $h = O(10^{-34})$. For $r = 0.2$, e.g., $1/\delta = 0.026$ gives a non-negligible $\langle S^z_{\rm imp}\rangle \simeq 0.13$. For $J \to J_c^-$, it is thus impractical to simulate spontaneous symmetry breaking.

[46] A. Georges, G. Kotliar, W. Krauth, and M. J. Rozenberg, Rev. Mod. Phys. **68**, 13 (1996).

[47] P. Coleman, *Introduction to Many-Body Physics* (Cambridge Univ. Press, Cambridge, UK, 2015).

[48] I. Peschel, J. Phys. A: Math. and Theor. **36**, L205 (2003).

[49] P. Calabrese and J. Cardy, J. Stat. Mech: Theor. and Exp. **2004**, P06002 (2004).

[50] F. B. Anders and A. Schiller, Phys. Rev. Lett. **95**, 196801 (2005).

[51] F. B. Anders and A. Schiller, Phys. Rev. B **74**, 245113 (2006).